| | **Experiment title:** Further investigations on Hg speciation in tree barks | **Experiment number**: EV-294 |
|---|---|---|
| **ESRF** | | |
| **Beamline**: BM16 | **Date of experiment**: from: 5/12/2018 to: 10/12/2018 | **Date of report**: 20/02/2020 |
| **Shifts:** 15 | **Local contact(s)**: Mauro Rovezzi | *Received at ESRF:* |

**Names and affiliations of applicants** (* indicates experimentalists):

Valentina Rimondi*, Earth Science Dept., University of Firenze

Fabrizio Bardelli*, CNR-Nanotec, c/o Department of Physics, University of La Sapienza

Francesco Di Benedetto, Earth Science Dept., University of Firenze

Pilario Costagliola, Earth Science Dept., University of Firenze

Marco Benvenuti, Earth Science Dept., University of Firenze

Laura Chiarantini, Earth Science Dept., University of Firenze

**Report:** *In this study, XAS analysis was used to identify Hg speciation in tree barks and soils collected from the Mt. Amiata Hg district (southern Tuscany, Italy). Mining activity in this area ceased in the 1980s, but Hg is widespread in soil, sediments, fish and air ([1] and references therein). A previous speciation study on tree barks was conducted in this area [2], but actually left a number of open questions. In the present study a consistent number of tree barks was investigated from the surface to the more internal layers (up to 3 cm depth) of bark tissues. Mercury inorganic species dominate at the bark-air interface, while a progressive increase of Hg-organic species is observed at depth.*

XAS measurements were conducted at BM16-FAME-UHD at the Hg $L_{III}$-edge (12284 eV) on tree (*Pinus nigra*) barks contaminated with Hg, and the related contaminated soil. For barks, different layers were investigated at increasing distance from the bark-atmosphere interface. In total, we investigated 5 tree barks (3 or 4 layer each for a total of 17 samples), and the associated 5 soils. All samples' spectra were measured in fluorescence yield detection mode with analyzer crystals. The Hg Lα1 ($3d_{5/2} \rightarrow 2p_{3/2}$) fluorescence line was selected using the 555 reflection of five spherically bent (radius 1 m) Si analyzer crystals (diameter 100 mm), aligned at an 81.8° Bragg angle in a vertical Rowland geometry. Spectra were collected in vacuum, and at low temperature (~10°K) to avoid possible photon-induced redox reactions. Al–filters of suitable thickness were used to attenuate the strong fluorescence signal from the matrix, especially from Fe when soils were studied. Depending on the concentration of Hg, 4 or 8 consecutive scans were acquired to improve statistics (half an hour each). Portions of the same samples used for chemical characterization were newly ground for synchrotron analysis in an agate mortar, then mixed and homogenized with cellulose, and finally pressed into a pellet. This procedure should ensure a homogenous distribution of Hg in the analyzed samples. Mercury references included: i) Hg sulphides (α-HgS, β-HgS species which may derive from direct volatilization of Hg-rich substrata in the surroundings (such as calcines); ii) Hg species which may derive from the binding of Hg with the bark organic matter, such as Hg(II)cysteine, Hg(II)phenol, Hg(SR)$_2$, and Hg(SR)$_3$. Other Hg references were kindly provided by Dr. Isaure (acquired at BM16-FAME-UHD). Principal Component Analysis (PCA) and Least Combination Fitting (LCF) were applied to the XANES spectra to obtain quantitative information on the sample speciation. LCF consists of a weighted linear combination of the reference standards suggested by PCA able to reconstruct a given experimental spectrum. PCA and LCF were
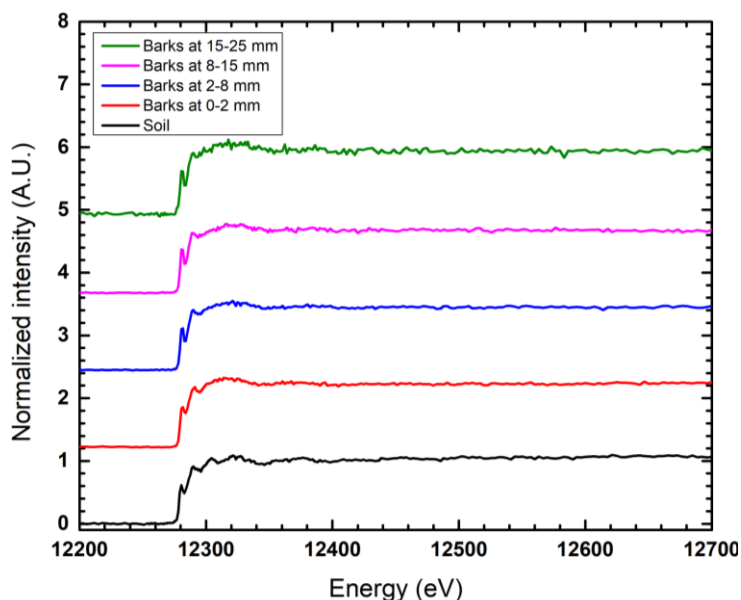
Fig. 1. XANES spectra of the bark sample A13 (different depths) and A13 soil.

performed using the SIXPACK and IFEFFIT packages, respectively [3,4]. As an example, we report the spectra of the A13 bark sample (4 depths) and related soil in Fig. 1.

In table 1, we report the LCF data on 3 tree barks (4 depths each). As clearly noted Hg speciation is dominated by inorganic Hg species (metacinnabar, β-HgS) at surface ($\geq$ 50%), while a progressive increase in Hg-organic species (Hg-thiolates, Hg bound to tannic acid, Hg-cystene, and $CH_3HgCl$) is found at depth.

Table 1. LCF data on tree barks.

| Sample | β-HgS % | Hg-$(SR)_2$/ Hg-$(SR)_3$ % | Hg-cyst % | tannic Hg/ $CH_3HgCl$ % | Σ | $\chi^2.10^4$ |
|---|---|---|---|---|---|---|
| A13_150_0-2mm | 59 | 41 | | | 100 | 2.5 |
| A13_150_2-8mm | 11 | 30 | 30 | 32 | 100 | 1.6 |
| A13_150_8-15mm | | 30 | 33 | 38 | 100 | 3.4 |
| A13_150_15-25mm | | 49 | 39 | 11 | 100 | 9.1 |
| A49_150_0-2mm bis | 47 | 39 | 64 | 14 | 100 | 5.8 |
| A49_150_2-6mm | 17 | 37 | 13 | 34 | 102 | 3.6 |
| A49_150_6-13mm | 10 | 37 | 22 | 32 | 101 | 3.3 |
| A49_150_13-27mm | | 35 | 30 | 36 | 101 | 16 |
| A22_150_0-2mm | 53 | | 46 | | 99 | 4.8 |
| A22_150_2-9mm | 43 | 26 | 20 | 11 | 100 | 6.0 |
| A22_150_9-15mm | 19 | 30 | 22 | 30 | 101 | 12 |
| A22_150_15-25mm | 22 | 32 | 26 | 20 | 101 | 23 |

| Sample | β-HgS % | α-HgS % | Σ | $\chi^2.10^4$ |
|---|---|---|---|---|
| A13_soil | 55 | 44 | 99 | 1.9 |
| A49_soil | 28 | 71 | 99 | 2.2 |
| A22_soil | 100 | | 100 | 2.9 |
| A19_soil | 72 | 27 | 99 | 4.3 |
| A11_soil | 32 | 68 | 100 | 0.8 |

Table 2. LCF data on soils.

On the contrary, soils are all composed by inorganic species, i.e. cinnabar and metacinnabar (Table 2). Metacinnabar is a common Hg species found in Mt. Amiata (and elsewhere) waste calcines [5], derived from the roasting of the primary cinnabar ore for Hg production. This mineral phase is indeed formed at high T (>450°C), and stabilized at low temperature due to impurities in the crystal lattice. Data from this study corroborate the previous findings recently published by [2]. In details, we can affirm that: i) suspended contaminated soil, containing inorganic Hg species, is deposited on the external bark layer, ii) Hg is progressively bound to the organic bark substratum by complexation with thiol- containing proteins and with COOH and OH groups of tannins.

**References** [1] Rimondi V., et al. (2015). Int. J. Geosci. **134**, 323-336; [2] Chiarantini L., et al. (2017) *Environm. Pollu.* **227**, 83-88. [3] Ravel, B., Newville, M., 2005. J. Synchrotron Radiat. **12**, 537−541.[4] Webb, S.M., 2005. Phys. Scr. **T115**, 1011−1014. [5] Rimondi V., et al. (2014) *Chem. Geol.* **380**, 110-118.